Use of Flow Modeling to Optimize the Twin-Screw Extrusion Process for the Preparation of Lignocellulosic Fiber-Based Composites

Françoise Berzin, Chantal David, Bruno Vergnes

frontiers in Materials

ORIGINAL RESEARCH
published: 24 July 2020
doi: 10.3389/fmats.2020.00218

Use of Flow Modeling to Optimize the Twin-Screw Extrusion Process for the Preparation of Lignocellulosic Fiber-Based Composites

Françoise Berzin[1]*, *Chantal David*[2] and *Bruno Vergnes*[3]*

[1] FARE, University of Reims Champagne Ardenne, INRAE, Reims, France, [2] Sciences Computers Consultants, Saint-Étienne, France, [3] MINES ParisTech, PSL Research University, Sophia Antipolis, France

Thermoplastic polymers reinforced by lignocellulosic fibers are increasingly used to replace conventional composites based on carbon or glass fibers. These materials are generally prepared by dispersing the fibers into the polymer matrix by melt mixing in a twin-screw extrusion process. However, during the process, a significant breakage occurs, leading to a reduction in the length, and diameter of the bundles and/or individual fibers. As the mechanical properties of the composite depend, among other, on the fiber morphology, it is important to understand and control the breakage mechanisms during the compounding process. In this paper, we show how the use of a thermomechanical model of twin-screw extrusion coupled with evolution laws of the fiber dimensions makes it possible to calculate the variation in the length and the diameter of the fibers, according to the local values of the flow parameters (shear rate, residence time, temperature, etc.). It is thus possible to define the best processing conditions (screw speed, feed rate, and barrel temperature) or the best screw profile to limit fiber degradation and prepare composites with optimal properties.

Keywords: lignocellulosic fibers, extrusion, modeling, breakage, optimization

OPEN ACCESS

Edited by:
Patricia Krawczak, IMT Lille Douai, France

Reviewed by:
Jose Antonio Covas, University of Minho, Portugal
Margaret J. Sobkowicz, University of Massachusetts Lowell, United States

***Correspondence:**
Françoise Berzin
francoise.berzin@univ-reims.fr
Bruno Vergnes
bruno.vergnes@mines-paristech.fr

Specialty section:
This article was submitted to Polymeric and Composite Materials, a section of the journal Frontiers in Materials

Received: *15 May 2020*
Accepted: *15 June 2020*
Published: *24 July 2020*

Citation:
Berzin F, David C and Vergnes B (2020) Use of Flow Modeling to Optimize the Twin-Screw Extrusion Process for the Preparation of Lignocellulosic Fiber-Based Composites. Front. Mater. 7:218. doi: 10.3389/fmats.2020.00218

INTRODUCTION

Due to their interesting properties, such as lightness, low cost, biobased origin, and satisfactory mechanical properties, lignocellulosic fibers are increasingly used for the preparation of thermoplastic matrix composites (Mohanty and Drzal, 2005; Hodzic and Shanks, 2014; Campilho, 2015). For short fibers (a few mm long) and thermoplastic matrices, the preferred process is melt mixing, i.e., compounding followed by extrusion or injection molding. In a first step, the fibers are mixed with the polymer matrix to obtain composite pellets, generally using a twin-screw extruder. In a second step, these pellets are processed by extrusion or injection molding to obtain the desired final shape. During the compounding step, many problems arise: first, when subjected to high stresses and strains, the fibers break. Not only the length, but also the diameter, of the initial bundles or the individual fibers can be considerably reduced. Second, the dispersion of the fibers into the matrix may be heterogeneous, with the existence of agglomerates. Third, if the temperature rises above about 200°C, thermal degradation can occur (Tajvidi and Takemura, 2010). Therefore, it is clear that the control of the extrusion conditions (screw profile, screw rotation speed, feed rate, etc.) is essential to prepare composites with optimal properties.

The role of the processing conditions on the fiber state and on the final properties of composites has been studied by many authors (Iannace et al., 2001; Le Baillif and Oksman, 2009; Quijano-Solis et al., 2009; Barkoula et al., 2010; Mano et al., 2010; Beaugrand and Berzin, 2012; El Sabbagh et al., 2014; Gonzalez-Sanchez and Gonzalez-Quesada, 2015; Feldmann et al., 2016). In recent years, we have developed a systematic study of the breakage of lignocellulosic fibers under thermomechanical stresses, based on rheo-optical observations (Le Duc et al., 2011; Castellani et al., 2016), and experiments carried out in internal mixers (Di Giuseppe et al., 2017) and twin-screw extruders (Berzin et al., 2017, 2018, 2019, 2020). These studies were conducted with different thermoplastic matrices (polypropylene and polybutylene succinate) and various lignocellulosic fibers (flax, hemp, sisal, miscanthus, and pineapple leaf fibers). The main result is that fiber breakage (i.e., reduction in the length and diameter of bundles and individual fibers) occurs primarily by fatigue, after numerous bends, unlike glass fibers which, due to their rigidity, break when a critical stress is reached (Durin et al., 2013). Consequently, the parameter which controls the kinetics of breakage is the strain accumulated by the fiber during the flow along the twin-screw extruder. This mechanism depends obviously on the properties of the fiber (plant origin, composition, water content, etc.) but also on its dimensions (longer fibers break more easily than short ones) and on the properties of the matrix (viscosity, affinity with fiber, etc.).

As the reinforcing properties of the fibers in the composite are among other controlled by their length (or their aspect ratio), it is necessary to limit breakage during compounding by twin-screw extrusion. However, it remains long and difficult by trial and error to find the optimal conditions, providing the maximum output while preserving the fiber length. In this paper, we will show how the use of flow modeling may allow to solve this delicate problem and to rapidly test many different solutions to select the most interesting.

MATERIALS AND METHODS

Composite Preparation

As noted in the introduction, we focus on the compounding step, where the fibers are dispersed into the matrix by using a co-rotating twin-screw extruder. The laboratory scale extruder used by Berzin et al. (2017) (Clextral BC21, Firminy, France) was selected as an example of application. It has a diameter of 25 mm and a length of 900 mm. The screw profile is shown in **Figure 1**. It comprises nine barrel elements (numbered from 1 to 9, from the hopper to the screw end) and, in addition to the screw conveying elements, it includes a left-handed element in zone 3 to melt the polymer matrix and two mixing blocks in zones 6 and 8, to disperse the fibers. The first one has five kneading discs, staggered by 90°, while the second one is more restrictive, with five kneading discs staggered by −45°. The matrix is introduced in zone 1, melted in the left-handed element (zone 3), then the fibers are added in zone 4.

The matrix is that used in the paper by Berzin et al. (2017). It is a mix of polypropylene (PP) and maleic anhydride grafted polypropylene (PP-g-MA) used as compatibilizer. Indeed, PP-g-MA is commonly used to improve the affinity between the hydrophilic fibers and the hydrophobic matrix (Feng et al., 2001; Bos et al., 2006). The PP-g-MA/fiber ratio is 1/10 by weight, as recommended in the literature (Le Moigne et al., 2011). Among the various fibers studied by Berzin et al. (2017), we have selected flax fibers for this paper. They were provided by FRD© company (Fibres Recherche Développement, Troyes, France) and have the following average dimensions: length $L = 4$ mm, diameter $D = 242\,\mu$m, aspect ratio $L/D = 18.8$. They contain 86.5 wt% of cellulose, 8.6 wt% of hemicellulose and 4.9 wt% of lignin.

Breakage Mechanisms

As indicated in the Introduction, the breakage mechanisms of flax fibers have been characterized and quantified in previous studies (Berzin et al., 2017; Di Giuseppe et al., 2017). For a fixed composition (type of fiber and matrix), it has been shown that the length L and the diameter D vary with the cumulated strain Γ, according to exponential functions. Local strain (without dimension) is the product of the local shear rate by the corresponding local residence time. It is then cumulated from the introduction of the fibers into the extruder up to the sampling point considered. The following expressions have been proposed and validated for various types of fibers and matrices (Berzin et al., 2017, 2018, 2019, 2020):

$$L = L_\infty + (L_0 - L_\infty)\exp(-k_L\,\Gamma) \quad (1)$$

$$D = D_\infty + (D_0 - D_\infty)\exp(-k_D\,\Gamma) \quad (2)$$

where L_0 (respectively, D_0) is the initial fiber length (respectively, diameter), L_∞ (respectively, D_∞) is its ultimate length (respectively, diameter), Γ is the cumulated strain and k_L (respectively, k_D) is a constant, quantifying the breakage kinetics. These constants depend on the properties of the fiber and the matrix. In the case of selected 4 mm flax fibers, the following values were obtained by Berzin et al. (2017): $L_0 = 4$ mm, $L_\infty = 1.2$ mm and $k_L = 1.1 \times 10^{-3}$, and $D_0 = 242\,\mu$m, $D_\infty = 100\,\mu$m, and $k_D = 2.8 \times 10^{-3}$. The corresponding experimental data and the theoretical curves provided by Equations (1) and (2) are illustrated in **Figure 2**.

Flow Modeling

The strain cannot be measured experimentally on a twin-screw extruder. Therefore, it is mandatory to use a model to calculate it and to assess changes in length and diameter of the fibers during the process. In this paper, the Ludovic® software developed by Vergnes et al. (1998) and marketed by SCC company (Saint Etienne, France) was used. Ludovic® is a model based on continuum mechanics, which solves the Stokes and energy equations within the framework of simplified geometry and kinematics. It simulates the whole extrusion process, from the introduction of solid polymer pellets in the hopper to the die exit, and calculates the variations along the screws of the main flow parameters, such as pressure, temperature, residence time, shear rate, stress, strain, etc. The simulation is based on a one-dimensional analysis. The screws are divided into elementary

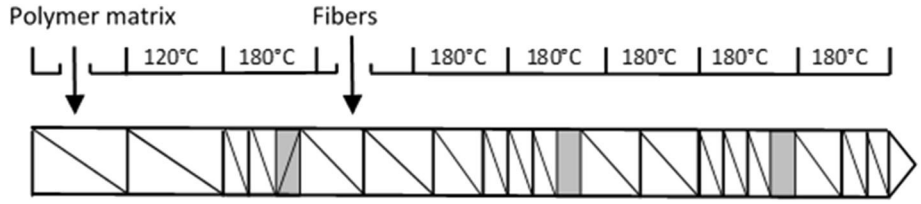

FIGURE 1 | Screw profile. The restrictive elements are in gray.

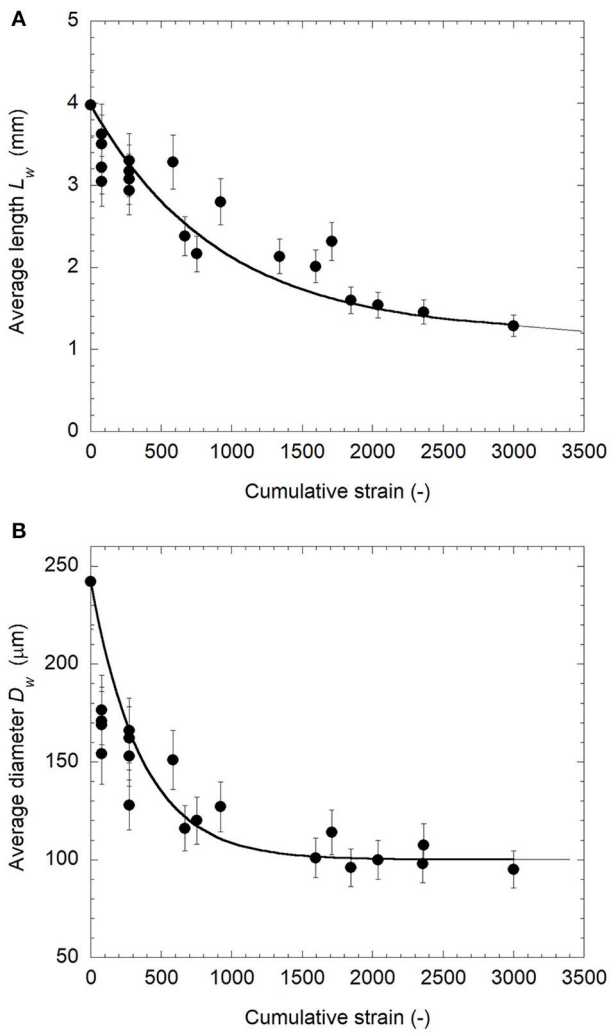

FIGURE 2 | Changes in length **(A)** and diameter **(B)** of 4 mm flax fibers as a function of cumulative strain. Symbols are experimental points, the lines are fits using (Equations 1, 2). Reprinted from Berzin et al. (2017) with permission.

sub-elements in which mass and thermal balances are written. In each type of element (left- and right-handed screw elements, blocks of kneading discs, etc.), average values of flow parameters are computed. The computation starts at the die exit and, element by element, temperature, and pressure are computed by an iterative backward procedure. We refer to the previous publication by Vergnes et al. (1998) for more details. For 20 years, the Ludovic® software has been extensively validated, experimentally (Carneiro et al., 2000) and by comparisons with more elaborate 3D models (Durin et al., 2014).

Optimization Procedure

The objective is to define the best processing conditions to prepare composites with the screw profile presented in **Figure 1**, based on the products defined in section Composite Preparation, i.e., a PP/PP-g-MA matrix reinforced by 20 wt% of flax fibers. The best conditions mean reaching the maximum flow rate while keeping the fibers as long as a possible, i.e., at the lowest cumulated strain. However, other constraints must be taken into account.

As explained in the Introduction, the fibers must be correctly distributed into the matrix. There are many indices to characterize the distributive mixing, but the simplest is to consider the variance σ^2 of the residence time distribution (RTD) (Manas-Zloczower, 2009). The RTD is usually represented by a function $E(t)$ which gives the extruder response to an input pulse (Danckwerts, 1953). By definition, $E(t)dt$ is the fraction of material leaving the extruder with a residence time between t and $t + dt$. It is such as:

$$\int_0^\infty E(t)dt = 1 \tag{3}$$

The mean residence time $\bar{t}$ is the first moment of the distribution:

$$\bar{t} = \int_0^\infty tE(t)dt \tag{4}$$

The variance σ^2 is the second moment centered on the mean:

$$\sigma^2 = \int_0^\infty (t - \bar{t})^2 E(t)dt \tag{5}$$

σ^2 represents the width of the RTD. In extrusion, it is directly linked to the intensity of the back-mixing. As an example for the application illustrated below, an arbitrary value has been chosen, i.e., a variance >200 s^2 will be requested.

To avoid thermal degradation, the maximum temperature encountered during the process should not exceed 200°C (Gassan

and Bledzki, 2001). As for the strain, this maximum value cannot be measured as it can be reached somewhere inside the extruder, typically in a block of kneading disc. Again, modeling is necessary to obtain this information.

Finally, the last constraint is the maximum loading that can be fed to the extruder. In practice, the fiber feeding is a real challenge because of their very low apparent density, close to 0.1, leading to a large volume to introduce. The maximum feeding capacity can be estimated as follows. The free cross section of the extruder S in the feeding zone can be written:

$$S = S_B - 2S_S \tag{6}$$

where S_B is the cross section of the eight-shaped barrel and S_S that of the screw. S_B and S_S can be easily calculated using the expressions proposed by Booy (1978):

$$S_B = 2(\pi - \psi)R_e^2 + C_l R_e \sin\psi \tag{7}$$

$$S_S = n\left[\psi C_1^2 - C_1 R_e \sin\psi\right] + \frac{n\alpha}{2}\left[R_e^2 + (C_l - R_e)^2\right] \tag{8}$$

where R_e is the screw radius, C_l is the centerline distance, n is the number of flights, and ψ and α are two angles, respectively, defined as:

$$\cos\psi = \frac{C_l}{2R_e} \tag{9}$$

$$\alpha = \frac{\pi}{n} - 2\psi \tag{10}$$

The free cross section S moves downstream at a velocity V equal to:

$$V = \frac{NB}{60} \tag{11}$$

where N is the screw speed (expressed in rpm) and B the screw pitch.

The theoretical free volume by time unit is then $Vol = S\frac{NB}{60}$. However, as the fibers fall out of the hopper, not all of this volume is directly accessible. Only the upper part of the cross section of the channel can be reached by the fibers. Moreover, part of the channel is already filled by the molten polymer. We can thus estimate that the real free volume is only about a third of the theoretical one. This approximation is sufficient because we are simply looking for an order of magnitude, not an exact value. It was checked that this order of magnitude agreed with the experimental observations. The maximum mass flow rate of the fibers will then be approximated as:

$$Q_{f\,\max} \approx \rho_a S\frac{NB}{180} \tag{12}$$

where ρ_a is the apparent density of the fibers, typically close to 0.1.

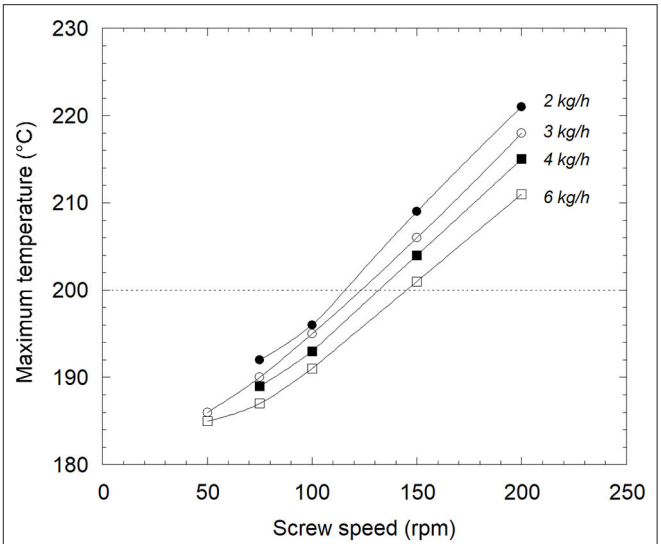

FIGURE 3 | Changes in maximum temperature with screw speed for different feed rates.

To summarize, the following constraints have to be respected for the optimization:

- maximum flow rate;
- minimum cumulated strain Γ;
- variance of RTD higher than 200 s^2;
- maximum temperature <200°C;
- fiber flow rate lower than $Q_{f\ \max}$.

RESULTS AND DISCUSSION

The optimization we propose is not a formal optimization, using specific algorithms, as we have done in other publications (Gaspar-Cunha et al., 2005, 2011), but a practical one, allowing to quickly define an optimal processing window. It will be conducted in two steps. First, the best processing conditions will be defined for the screw in **Figure 1**, according to the constraints defined in section Optimization Procedure. Second, we will show how changing the screw profile can help to improve the first results.

Optimization of Processing Conditions

To define the best processing conditions, simulations with Ludovic® software are performed by varying the total flow rate (PP/PP-g-MA + 20 wt% flax fibers) from 2 to 6 kg/h and the screw speed from 50 to 200 rpm. For each simulation, the values of the cumulated strain Γ, the RTD variance σ^2 and the maximum temperature $T_{\max}$ are recorded. The results are presented in **Figures 3–5**.

The maximum temperature $T_{\max}$ increases a lot with the screw speed, due to viscous dissipation (**Figure 3**). It can reach values of 30–40°C above the barrel temperature (180°C), capable of degrading not only the fibers but also the matrix. At a fixed screw speed, $T_{\max}$ decreases slowly with the feed rate. In order to

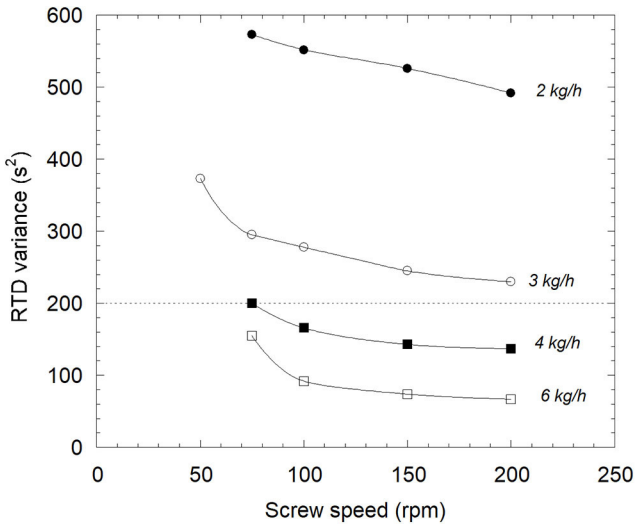

FIGURE 4 | Changes in RTD variance with screw speed for different feed rates.

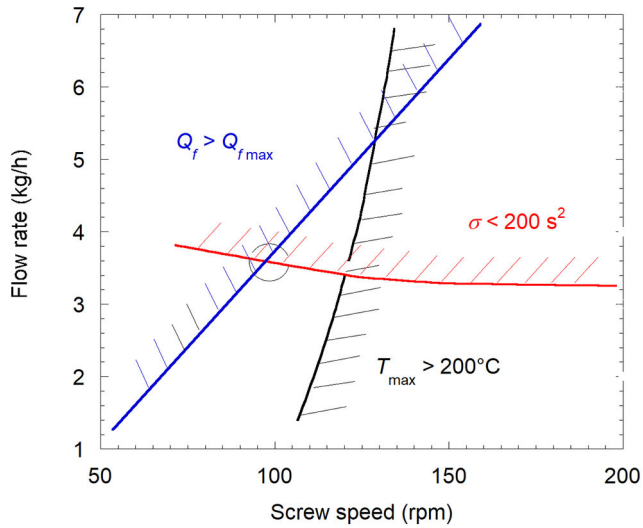

FIGURE 6 | Processing window on a screw speed/feed rate map. Hatched regions are forbidden by the various criteria.

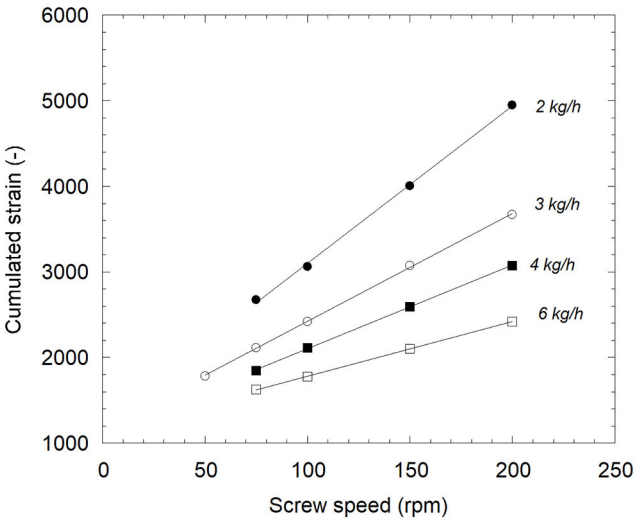

FIGURE 5 | Changes in cumulated strain with screw speed for different feed rates.

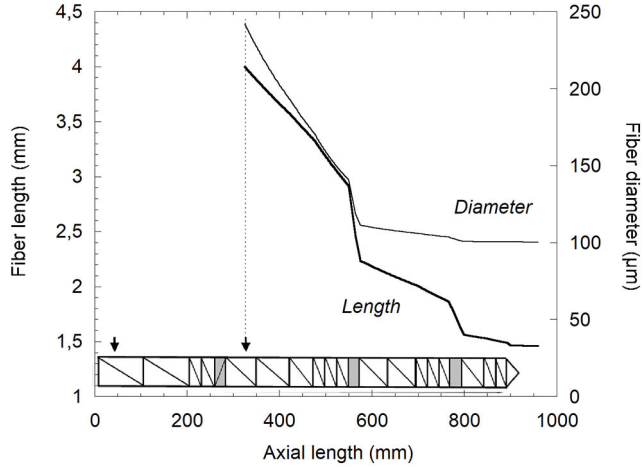

FIGURE 7 | Calculated changes in fiber length and diameter along the screw profile in the optimized conditions.

keep the temperature below the maximum value of 200°C, low screw speeds (in the range 110–150 rpm) are necessary.

The variance of the RTD σ^2, selected as the distributive mixing index, is shown in **Figure 4**. It decreases slightly with the screw speed, but is mainly affected by the flow rate. These effects of screw speed and feed rate on the RTD are well-known in twin-screw extrusion (Poulesquen and Vergnes, 2003): an increase in screw speed shifts the RTD toward shorter times, without affecting its shape, while an increase in feed rate also shifts the RTD toward shorter times, but mainly narrows its width. To comply with the constraint of RTD variance >200 s^2, low flow rates are mandatory: the limit appears between 3 and 4 kg/h.

Finally, the values of the cumulated strain Γ are presented in **Figure 5**. Γ increases linearly with the screw speed and decreases with the feed rate. Indeed, it can be shown that Γ is proportional to the ratio N/Q (Lafleur and Vergnes, 2014). Therefore, to limit the breakage of the fibers, it is necessary to favor low speeds and high feed rates.

If we consider these different results, it is clear that certain conditions appear to be contradictory. To have a clearer view of the situation, plots of isovalues of the limiting parameters T_{max}, σ^2, and $Q_{f\,max}$ are plotted on a flow rate/screw speed map (**Figure 6**). This shows that the processing windows is quite narrow: the screw speed is limited at 100–110 rpm by the maximum temperature and the flow rate below 4 kg/h by the RTD variance. Moreover, another limit is added by the

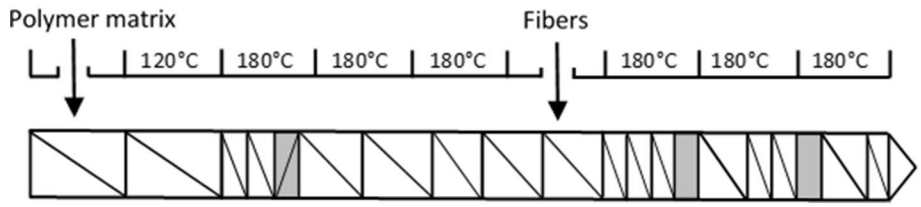

FIGURE 8 | Modified screw profile. The restrictive elements are in gray.

maximum feeding rate of the fibers. In conclusion, it appears that the optimal conditions (circle in **Figure 6**) are $Q = 3.6$ kg/h at $N = 95$ rpm. These values provide a maximum temperature of 194°C, reached in the second block of kneading discs, a RTD variance of 200 s^2, and a cumulated strain of 2,157. For these processing conditions, it is now possible to use (Equations 1, 2) to calculate the variations of the fiber dimensions along the screws. For example, **Figure 7** shows the change in fiber length and diameter under the optimized conditions. Fibers of 1.46 mm in length and 100 μm in diameter are obtained at the die exit.

Optimization of Screw Geometry

It can be seen in **Figure 7** that the fibers undergo a significant reduction in both the length and the diameter, even though the processing conditions have been optimized. Degradation occurs rapidly, along the first screw conveying elements, as soon as the fibers are introduced into the extruder. Therefore, to limit this problem and reduce the fiber attrition, the simplest way is to move the fiber introduction and the two blocks of kneading discs downstream, as shown in **Figure 8**. However, a certain distance along the screws remains necessary to ensure a good distribution of the fibers into the matrix. By repeating the same procedure as in the previous paragraph (different flow simulations under various conditions of screw speed and feed rate) and with the same constraints (on T_{max}, σ^2, and Q_{fmax}), the processing window for this new configuration can be established. The optimal conditions are very close to those of the first profile, with a flow rate of 3.6 kg/h and a screw speed of 100 rpm. However, as the fibers are introduced later, the cumulated strain is lower, here 1,820, and, as expected, the fibers are a little longer: 1.58 mm (i.e., a gain of 8%). Nevertheless, the improvement is not really significant and further modifications to the geometry would be necessary for better results. As the main limitation of the flow rate is the RTD variance, we can imagine to increase this parameter by increasing the length of the first block of kneading discs, staggered at 90° (50 mm instead of 25 mm). In doing so, the numerical simulation shows that at 120 rpm and always with the same constraints, the feed rate can be increased up to 4.8 kg/h, i.e., a gain of 33%. However, the cumulated strain remains around 2,000, indicating no further improvement in the fiber length. Based on the previous results of Berzin et al. (2017), starting from initial longer fibers could be a solution: indeed, for flax fibers 12 mm long, the same processing conditions (4.8 kg/h, 120 rpm) would lead to final fibers about 3 mm in length.

CONCLUSION

In this paper, it has been shown that the use of a model of the flow along a twin-screw extruder coupled with evolution laws for the dimensions of lignocellulosic fibers can be a very useful tool for optimizing the preparation of natural fiber composites. In a very short time (each calculation requires only a few seconds on a PC), it allows one to test many possible conditions and, according to certain constraints, to optimize the processing conditions and the screw profile. Similarly, flow modeling could also be a privileged tool for solving the often difficult problem of scale-up, from laboratory to industrial scale.

DATA AVAILABILITY STATEMENT

The raw data supporting the conclusions of this article will be made available by the authors, without undue reservation.

AUTHOR CONTRIBUTIONS

FB, CD, and BV contributed equally to the paper, by performing the simulations, discussing the results, and writing the text. All authors contributed to the article and approved the submitted version.

REFERENCES

Barkoula, N. M., Garkhail, S. K., and Peijs, T. (2010). Effect of compounding and injections molding on the mechanical properties of flax fiber polypropylene composites. *J. Reinf. Plast. Comp.* 29, 1366–1385. doi: 10.1177/0731684409104465

Beaugrand, J., and Berzin, F. (2012). Lignocellulosic fiber reinforced composites: influence of compounding conditions on defibrization and mechanical properties. *J. Appl. Polym. Sci.* 128, 1227–1238. doi: 10.1002/app.38468

Berzin, F., Amornsakchai, T., Lemaitre, A., Castellani, R., and Vergnes, B. (2019). Influence of fiber content on rheological and mechanical properties of pineapple leaf fibers-polypropylene composites prepared by twin-screw extrusion. *Polym. Comp.* 40, 4519–4529. doi: 10.1002/pc.25308

Berzin, F., Amornsakchai, T., Lemaitre, A., Di Giuseppe, E., and Vergnes, B. (2018). Processing and properties of pineapple leaf fibers-polypropylene composites prepared by twin-screw extrusion. *Polym. Comp.* 39, 3817–4223. doi: 10.1002/pc.24475

Berzin, F., Beaugrand, J., Dobosz, S., Budtova, T., and Vergnes, B. (2017). Lignocellulosic fiber breakage in a molten polymer. Part 3. Modelling of the dimensional evolution of the fibers during compounding by twin screw extrusion. *Comp. Part A* 101, 422–431. doi: 10.1016/j.compositesa.2017.07.009

Berzin, F., Lemkhanter, L., Marcuello-Angles, C., Molinari, M., Chabbert, B., Aguié, V., et al. (2020). Influence of the polarity of the matrix on the breakage mechanisms of lignocellulosic fibers during twin-screw extrusion. *Polym. Comp.* 41, 1106–1117. doi: 10.1002/pc.25442

Booy, M. L. (1978). Geometry of fully wiped twin-screw equipment. *Polym. Eng. Sci.* 18, 973–984. doi: 10.1002/pen.760181212

Bos, H. L., Müssig, J., and van den Oever, M. J. A. (2006). Mechanical properties of short-flax-fibre reinforced compounds. *Comp. Part A* 37, 1591–1604. doi: 10.1016/j.compositesa.2005.10.011

Campilho, R. D. S. G. (2015). *Natural Fibers Composites.* Boca Raton, FL: CRC Press, 368. doi: 10.1201/b19062

Carneiro, O. S., Covas, J. A., and Vergnes, B. (2000). Experimental and theoretical study of the twin screw extrusion of polypropylene. *J. Appl. Polym. Sci.* 78, 1419–1430. doi: 10.1002/1097-4628(20001114)78:7<1419::AID-APP130>3.0.CO;2-B

Castellani, R., Di Giuseppe, E., Beaugrand, J., Dobosz, S., Berzin, F., Vergnes, B., et al. (2016). Lignocellulosic fiber breakage in a molten polymer. Part 1. Quantitative analysis using rheo-optical observations. *Comp. Part A* 91, 229–237. doi: 10.1016/j.compositesa.2016.10.015

Danckwerts, P. V. (1953). Continuous flow systems: distribution of residence times. *Chem. Eng. Sci.* 2, 1–13. doi: 10.1016/0009-2509(53)80001-1

Di Giuseppe, E., Castellani, R., Budtova, T., and Vergnes, B. (2017). Lignocellulosic fiber breakage in a molten polymer. Part 2. Quantitative analysis of the breakage mechanisms during compounding. *Comp. Part A* 95, 31–39. doi: 10.1016/j.compositesa.2016.12.011

Durin, A., De Micheli, P., Nguyen, H. C., David, C., Valette, R., and Vergnes, B. (2014). Comparison between 1D and 3D approaches for twin-screw extrusion simulation. *Intern. Polym. Proc.* 29, 641–648. doi: 10.3139/217.2951

Durin, A., De Micheli, P., Ville, J., Inceoglu, F., Valette, R., and Vergnes, B. (2013). A matricial approach of fibre breakage in twin-screw extrusion of glass fibres reinforced thermoplastics. *Comp. Part A* 48, 47–56. doi: 10.1016/j.compositesa.2012.12.011

El Sabbagh, A. M. M., Steuernagel, L., Meiners, D., and Ziegmann, D. (2014). Effect of extruder elements on fiber dimensions and mechanical properties of bast natural fiber polypropylene composites. *J. Appl. Polym. Sci.* 131:40435. doi: 10.1002/app.40435

Feldmann, M., Heim, H. P., and Zarges, J. C. (2016). Influence of the process parameters on the mechanical properties of engineering biocomposites using a twin-screw extruder. *Comp. Part A* 83, 113–119. doi: 10.1016/j.compositesa.2015.03.028

Feng, D., Caulfield, D. F., and Sanadi, A. R. (2001). Effect of compatibilizer on the structure-property relationships of kenaf-fiber/polypropylene composites. *Polym. Comp.* 22, 506–517. doi: 10.1002/pc.10555

Gaspar-Cunha, A., Covas, J. A., and Vergnes, B. (2005). Defining the configuration of co-rotating twin-screw extruders with multiobjective evolutionary algorithms. *Polym. Eng. Sci.* 45, 1159–1173. doi: 10.1002/pen.20391

Gaspar-Cunha, A., Covas, J. A., Vergnes, B., and Berzin, F. (2011). "Reactive extrusion - optimization of representative processes," in *Optimization of Polymer Processing*, eds A. Gaspar-Cunha and J. A. Covas (New York, NY: Nova Science Publishers), 115–143.

Gassan, J., and Bledzki, A. K. (2001). Thermal degradation of flax and jute fibers. *J. Appl. Polym. Sci.* 82, 1417–1422. doi: 10.1002/app.1979

Gonzalez-Sanchez, C., and Gonzalez-Quesada, M. (2015). Novel automated method for evaluating the morphological changes of cellulose fibres during extrusion-compounding of plastic-matrix composites. *Comp. Part A* 69, 1–9. doi: 10.1016/j.compositesa.2014.10.026

Hodzic, A., and Shanks, R. (2014). *Natural Fibre Composites, Material, Processes and Properties.* Cambridge: Woodhead Publishing, 408.

Iannace, S., Ali, R., and Nicolai, L. (2001). Effect of processing conditions on dimensions of sisal fibers in thermoplastic biodegradable composites. *J. Appl. Polym. Sci.* 79, 1084–1091. doi: 10.1002/1097-4628(20010207)79:6<1084::AID-APP120>3.0.CO;2-J

Lafleur, P. G., and Vergnes, B. (2014). *Polymer Extrusion*. London: ISTE-Wiley, 337. doi: 10.1002/9781118827123

Le Baillif, M., and Oksman, K. (2009). The effect of processing on fiber dispersion, fiber length, and thermal degradation of bleached sulfite cellulose fiber polypropylene composites. *J. Therm. Comp. Mat.* 22, 115–133. doi: 10.1177/0892705708091608

Le Duc, A., Budtova, T., and Vergnes, B. (2011). Polypropylene/natural fibres composites: analysis of fibre dimensions after compounding and observations of fibre rupture by rheo-optics. *Comp. Part A* 42, 1727–1737. doi: 10.1016/j.compositesa.2011.07.027

Le Moigne, N., van den Oever, M., and Budtova, T. (2011). A statistical analysis of fibre size and shape distribution after compounding in composites reinforced by natural fibres. *Comp. Part A* 42, 1542–1550. doi: 10.1016/j.compositesa.2011.07.012

Manas-Zloczower, I. (2009). *Mixing and Compounding of Polymers – Theory and Practice.* Munich: Hanser, 1158. doi: 10.3139/97834464 33717

Mano, B., Araujo, J. R., Spinace, M. A. S., and De Paoli, M. A. (2010). Polyolefin composites with curaua fibres: effect of the processing conditions on mechanical properties, morphology and fibres dimensions. *Comp. Sci. Tech.* 70, 29–35. doi: 10.1016/j.compscitech.2009.09.002

Mohanty, A. K., and Drzal, L. T. (2005). *Natural Fibres, Biopolymers and Biocomposites*. Boca Raton, FL: CRC Press, 896. doi: 10.1201/9780203508206.ch1

Poulesquen, A., and Vergnes, B. (2003). A study of residence time distribution in co-rotating twin screw extruders. Part I: theoretical modelling. *Polym. Eng. Sci.* 43, 1841–1848. doi: 10.1002/pen.10156

Quijano-Solis, C., Yan, N., and Zhang, S. Y. (2009). Effect of mixing conditions and initial fiber morphology on fiber dimensions after processing. *Comp. Part A* 40, 351–358. doi: 10.1016/j.compositesa.2008.12.014

Tajvidi, M., and Takemura, A. (2010). Thermal degradation of natural fiber-reinforced polypropylene composites. *J. Therm. Comp. Mat.* 23, 281–298. doi: 10.1177/0892705709347063

Vergnes, B., Della Valle, G., and Delamare, L. (1998). A global computer software for polymer flows in corotating twin screw extruders. *Polym. Eng. Sci.* 38, 1781–1792. doi: 10.1002/pen.10348

Conflict of Interest: CD was employed by the company SCC.

The remaining authors declare that the research was conducted in the absence of any commercial or financial relationships that could be construed as a potential conflict of interest.